ACS OMEGA

http://pubs.acs.org/journal/acsodf

Article

Immobilization of Lipase from *Thermomyces lanuginosus* in Magnetic Macroporous ZIF-8 Improves Lipase Reusability in Biodiesel Preparation

Yuhan Li, Hao Zhou, Lingmei Dai, Dehua Liu, Sulaiman Al-Zuhair,* and Wei Du*

Cite This: *ACS Omega* 2022, 7, 274–280

Read Online

ACCESS | Metrics & More | Article Recommendations

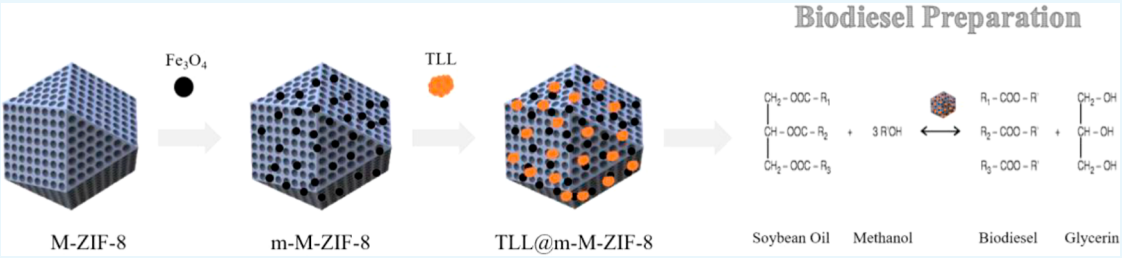

ABSTRACT: In recent years, metal−organic frameworks (MOFs) have emerged as a promising support for immobilizing enzymes due to their high designability and structural diversity. Previous studies show that MOFs with single-crystal-ordered macroporous structures can effectively improve the accessibility of large-size enzyme and reduce the mass transfer resistance compared to conventional MOFs. In order to further enhance the reusability of lipase immobilized on macroporous MOFs, modification of MOFs through some magnetic particles could be an efficient approach. In this work, magnetic macroporous zeolitic imidazolate framework-8 (ZIF-8), referred to as m-M-ZIF-8 (with an average macropore size of about 140 nm), was synthesized and used for the immobilization of *Thermomyces lanuginosus* lipase (TLL). It was found that enzyme loading and the specific enzyme activity of the immobilized lipase were greatly enhanced through this magnetic modification. The enzyme loading of TLL@C-ZIF-8, T LL@M-ZIF-8, and TLL@m-M-ZIF-8 was 0.060, 0.074, and 0.076 mg/mg respectively. Besides, the activity of 93.5% was maintained after the immobilized lipase being repeatedly used for five batches, which was much higher than that of the immobilized lipase without magnetic modification, which was only 73.4%.

1. INTRODUCTION

In recent years, metal−organic frameworks (MOFs) have been considered as a promising support material for immobilizing enzymes with great potential, owing to their designability and high structural diversity. Through rational design and easy post-synthesis modification, the performances of MOF-immobilized enzymes were enhanced greatly in many cases.[1,2] For instance, MOF-immobilized formate dehydrogenase and horse radish peroxidase showed higher stability and catalytic activity.[3,4]

Despite the fact that MOFs with large surface areas and tunable porosity could be excellent supports for immobilizing enzymes, small crystalline pore sizes (usually lower than 5 nm) would limit their application in enzymes' immobilization because the molecular size of some enzymes (like lipase) is usually larger than the pore size of MOFs.[5−7] In 2018, macroporous zeolitic imidazolate framework-8 (M-ZIF-8) was proposed and successfully prepared by Shen et al.[8] This provides a new platform for immobilizing enzymes inside macroporous MOFs. It was found that *Aspergillus niger* lipase immobilized inside macroporous ZIF-8 (M-ZIF-8) has higher enzymatic activity (6.5 folds), activity recovery (3.8 folds), and thermal stability (1.4 and 3.4 at 80 and 100 °C, respectively) as compared to free enzyme.[5] The similar good results were also achieved in the hydrolysis of macroporous ZIF-8-immobilized lipase.[9]

Although immobilizing enzymes inside macroporous MOFs can enhance their properties, the difficulty in recovering the immobilized enzymes (mostly in powder form) limits their practical application to a great extent.[10] MOFs combined with magnetic nanoparticles for enzyme immobilization might be a promising strategy to solve this problem. It was reported that MOFs modified with Fe_3O_4 nanoparticles were used for the immobilization of α-L-rhamnosidase (RHA), and the immobi-

Received: August 23, 2021
Accepted: December 16, 2021
Published: December 29, 2021

© 2021 The Authors. Published by American Chemical Society

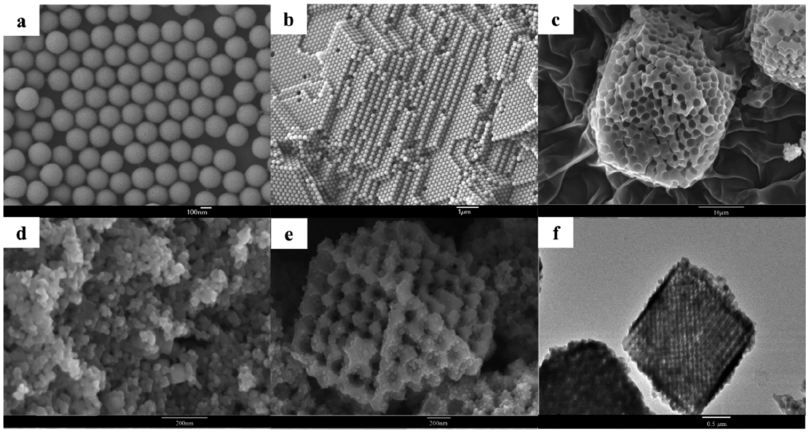

Figure 1. SEM images of (a) PS nanoparticles, (b) PS template, (c) M-ZIF-8, (d) Fe_3O_4 nanoparticles, and (e) m-M-ZIF-8 and (f) TEM image of M-ZIF-8.

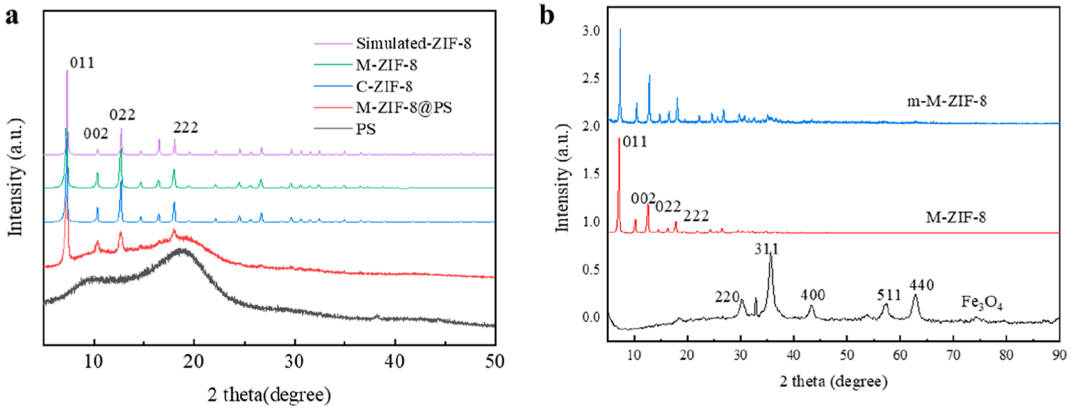

Figure 2. (a) XRD patterns of simulated-ZIF-8, M-ZIF-8, C-ZIF-8, M-ZIF-8@PS, and PS. (b) XRD patterns of m-M-ZIF-8, M-ZIF-8, and Fe_3O_4.

lized enzyme (Rha@m-MOF) showed a significantly enhanced reusability.[11] The catalytic efficiency of lipase@m-ZIF-8 was 2.48 times higher than that of free lipase, and it had stronger tolerance toward organic solvents.[12]

So far, most studies regarding magnetic modification are mostly related to microporous/mesoporous MOFs, and few studies are about macroporous MOFs' modification through nano-magnetic particles, especially in the field of enzyme immobilization.[13] In this paper, we worked on synthesizing cystal-ordered macroporous ZIF-8, followed by modification through Fe_3O_4 nanoparticles to obtain the magnetic M-ZIF-8 (referred to as m-M-ZIF-8). This m-M-ZIF-8 was further adopted to immobilize *Thermomyces lanuginosus* lipase (TLL). Finally, the immobilized lipase TLL@m-M-ZIF-8 was used for biodiesel production, and the related performance was investigated.

2. RESULTS AND DISCUSSION

2.1. Synthesis and Characterization of m-M-ZIF-8. The scanning electron microscopy (SEM) images of PS nanoparticles, PS template, M-ZIF-8, Fe_3O_4 nanoparticles, and m-M-ZIF-8 are presented in Figure 1a−e, and the TEM image of M-ZIF-8 is shown in Figure 1f. As shown in Figure 1a, the PS nanoparticles exhibited a uniform sphere shape with a diameter of about 200 nm. After centrifugation, the attained PS template showed a highly ordered structure (Figure 1b). As shown in Figure 1c,f, the macropores of M-ZIF-8 were observed clearly with an average diameter of about 140 nm. In addition, the mean grain size of Fe_3O_4 was about 30 nm (Figure 1d). Figure 1e shows that the structure of m-M-ZIF-8 had the structure of both M-ZIF-8 and Fe_3O_4 nanoparticles, and the diameter of m-M-ZIF-8 was around 2 μm.

The crystalline and micropore structure of the resulting M-ZIF-8, Fe_3O_4, and *m*-ZIF-8 was assessed by X-ray diffraction (XRD). As shown in Figure 2a, the XRD pattern of M-ZIF-8 is consistent with that of the simulated-ZIF-8 and conventional ZIF-8 (C-ZIF-8), which proved that the crystalline structure was maintained well during the synthesis procedure. Besides, the XRD patterns of M-ZIF-8, M-ZIF-8@PS, and PS (Figure 2a) illustrated the growth of M-ZIF-8 on PS templates and the etching of PS templates with tetrahydrofuran (THF). For m-M-ZIF-8, XRD patterns showed that m-M-ZIF-8 possessed the characteristic peaks of both M-ZIF-8 and Fe_3O_4 (Figure 2b), indicating that the crystalline structure of m-M-ZIF-8 was still retained well during the magnetization modification.

The Fourier transform infrared (FTIR) spectrum of m-M-ZIF-8, N-M-ZIF-8, M-ZIF-8, *N*-Fe_3O_4, and Fe_3O_4 are shown in Figure 3. The characteristic bands at 1310 and 1584 cm^{-1} were attributed to the Zn−N and imidazole ring stretching vibrations,[16] which illustrated the presence of ZIF-8 in m-M-ZIF-8, N-M-ZIF-8, and M-ZIF-8. The bands around 3300−3500 cm^{-1} indicated the existence of characteristic groups of amino acids, which proved the success of the amination modification of M-ZIF-8 and Fe_3O_4. The bands at 575 cm^{-1} were attributed to the Fe-O group,[13] indicating the presence of Fe_3O_4 in m-M-ZIF-8.

https://doi.org/10.1021/acsomega.1c04601
ACS Omega 2022, 7, 274−280

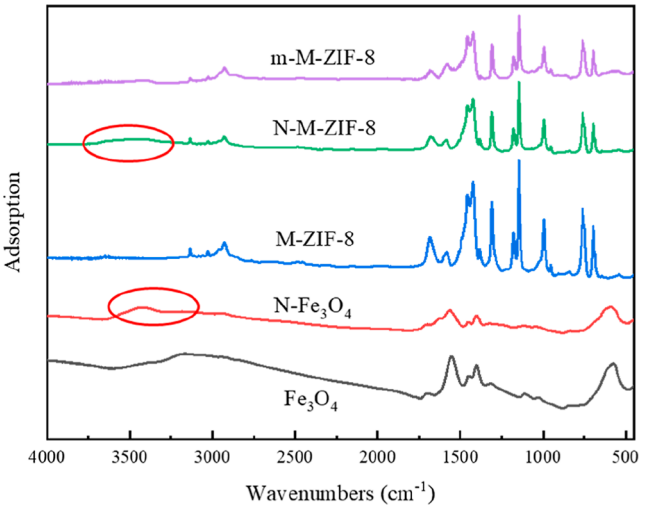

Figure 3. FTIR spectra of m-M-ZIF-8, N-M-ZIF-8, M-ZIF-8, *N*-Fe_3O_4, and Fe_3O_4.

N_2 adsorption−desorption isotherms of M-ZIF-8 and m-M-ZIF-8 are shown in Figure 4. The Brunauer−Emmett−Teller

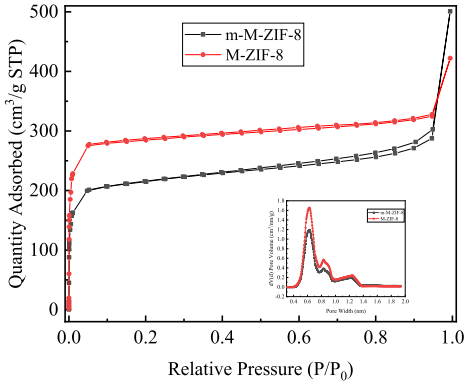

Figure 4. N_2 sorption isotherms of M-ZIF-8 and m-M-ZIF-8 at 77 K. The inset shows the corresponding micropore size distribution of M-ZIF-8 and m-M-ZIF-8 from the DFT model.

(BET) surface area and micropore volume of M-ZIF-8 were 867.523 cm^2/g and 0.437 cm^3/g, respectively. The BET surface area and micropore volume of m-M-ZIF-8 were 649.075 cm^2/g and 0.327 cm^3/g, respectively. It is observed that the magnetic modification caused a loss of part of the macroporous structure, which agrees with the results of Feng et al.[13] Besides, the micropore size distribution of m-M-ZIF-8 was found to be similar to that of M-ZIF-8, indicating that the microporous structure of m-M-ZIF-8 maintained well during the modification process.

The magnetization curves of Fe_3O_4, *N*-Fe_3O_4, and m-M-ZIF-8 are depicted in Figure 5. The curves show no obvious hysteresis for all tested particles. The superparamagnetic behavior of m-M-ZIF-8 made it easy to recycle it from the reaction system using a magnet.

2.2. Catalytic Performance of TLL@m-M-ZIF-8. TLL was physically adsorbed on M-ZIF-8 and m-M-ZIF-8 respectively through TLL directly diffusing into the macropores. As shown in Figure 6, both TLL@M-ZIF-8 and TLL@m-M-ZIF-8 showed significant improvements in terms of specific enzyme activity and activity recovery as compared to

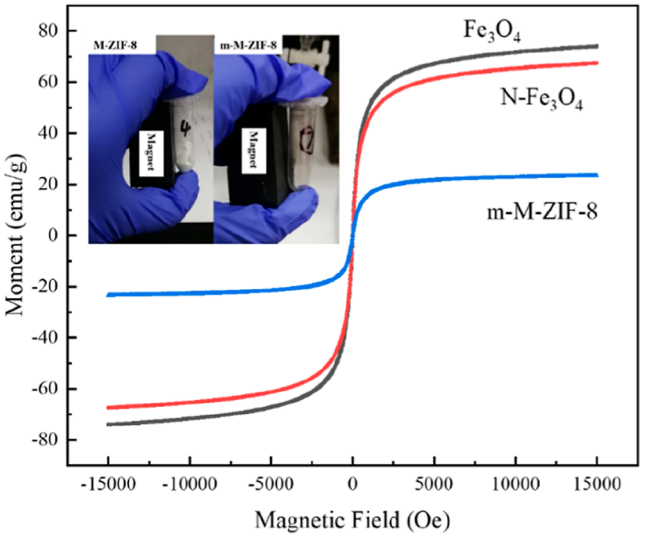

Figure 5. Magnetization curves of Fe_3O_4, *N*-Fe_3O_4, and m-M-ZIF-8.

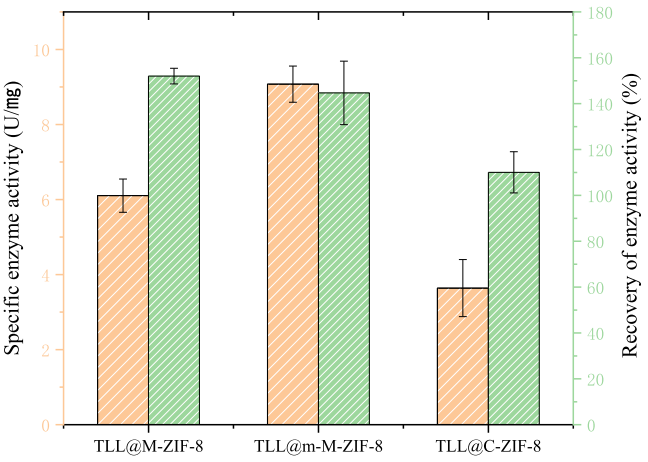

Figure 6. Specific enzyme activity (pink) and recovery of enzyme activity (green) of immobilized lipases.

TLL@C-ZIF-8. This was mainly due to the larger pore sizes of M-ZIF-8 and m-M-ZIF-8, which allows TLL molecules to penetrate into the macropores of around 140 nm, resulting in pore adsorption inside the macroporous ZIF-8. The enzyme loading (0.060 mg/mg for TLL@C-ZIF-8, 0.074 mg/mg for TLL@M-ZIF-8, and 0.076 mg/mg for TLL@m-M-ZIF-8) was also improved a lot by introducing the macroporous structure into ZIF-8. Compared to TLL@M-ZIF-8, TLL@m-M-ZIF-8 had a higher apparent specific enzyme activity, which might be due to the higher enzyme loading. M-ZIF-8 with magnetism modification displayed higher hydrophilicity than that of M-ZIF-8, leading to easy diffusion of enzyme molecules into the pores of m-M-ZIF-8. This might be attributed to its higher protein loading capacity and enzymatic activity recovery. The recovery of enzyme activity of TLL@m-M-ZIF-8 was similar to that of TLL@M-ZIF-8, illustrating that the magnetic modification did not have an inhibition effect on the enzyme. Besides, it was found that the recovery of enzyme activity of the three immobilized lipases was all higher than 100%, which might result from the strengthened interfacial activation of the lipase by introducing hydrophobic MOFs (M-ZIF-8, m-M-ZIF-8, and C-ZIF-8 are hydrophobic).[17]

https://doi.org/10.1021/acsomega.1c04601
ACS Omega 2022, 7, 274−280

2.3. Enhanced Reusability of TLL@m-M-ZIF-8 in Biodiesel Production. The catalytic performances of TLL@M-ZIF-8 and TLL@m-M-ZIF-8 in biodiesel production were investigated. For the first batch, the FAME (fatty acid methyl ester) yield using TLL@m-M-ZIF-8 as a biocatalyst reached 98.96% after 12 h of reaction, much higher than that of TLL@M-ZIF-8 (only 80.31%). This result could be attributed to the higher apparent specific enzyme activity of TLL@m-M-ZIF-8. These results agree with those of Feng et al.,[13] wherein the V_{max}/K_m value of enzyme immobilized on magnetic macroporous ZIF-8 was higher than that of the immobilized enzyme without magnetic modification.

The reusability test of TLL@M-ZIF-8 and TLL@m-M-ZIF-8 in biodiesel production was investigated, and the results are shown in Figure 7. It was found that TLL@m-M-ZIF-8 showed significantly higher reusability. After five batches of reaction, the relative activity of TLL@m-M-ZIF-8 was 93.50%, whereas that of TLL@M-ZIF-8 was only 73.39%. These results indicated that the magnetic modification greatly enhanced the reusability of immobilized lipase.

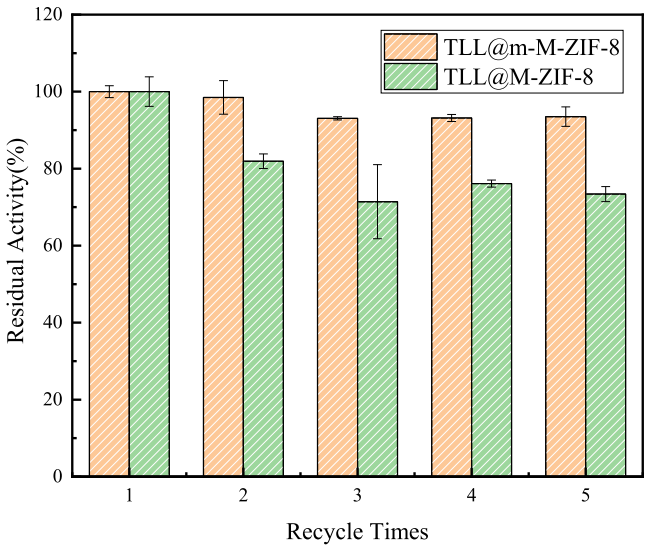

Figure 7. Reusability of TLL@M-ZIF-8 (green) and TLL@m-M-ZIF-8 (red).

3. MATERIAL AND METHODS

3.1. Materials. Free lipase (Eversa Transform 2.0, ET 2.0) from the genetically modified *T. lanuginosus* was obtained from Novozymes (Denmark). Tributyrin, THF, anhydrous methanol, and ethanol were purchased from Shanghai Titan technology co., Ltd, China. A bicinchoninic acid (BCA) protein assay kit was purchased from Beijing Dingguo Changsheng Biotechnology co. Ltd, China. Heptadecanoic acid methyl ester was purchased from Sigma-Aldrich (St. Louis, MO). Soybean oil was purchased from a local market. All the other chemicals obtained commercially were of analytical grade.

3.2. MOF Characterization. Powder XRD patterns were recorded using a Bruker D8 Advance X-ray diffractometer with a Cu Kα anode (λ = 1.5418 Å) at 40 kV and 40 mA. Fourier transform infrared (FTIR) patterns were conducted using a Nicolet 6700FTIR system with KBr as background. N_2 adsorption−desorption isotherms were measured at 77 K on a SI-MP analyzer from Beijing Kangta Technology Co., Ltd. The samples were degassed at 100 °C for 12 h before the measurements. Specific surface areas were calculated using the BET method in the relative pressure range P/P_0 = 0.05−0.30. Field-emission SEM images were obtained using JSM 7401F at an acceleration voltage of 5.0 kV and Merlin at an acceleration voltage of 1.0 kV. Transmission electron microscopy (TEM) images were obtained using JEM2010 at an operating voltage of 200 kV. The magnetic hysteresis regression curve was obtained on SQUID-VSM from Quantum Design, America.

3.3. Experimental Methods. *3.3.1. Preparation of a 3D Ordered PS Template.* A 3D ordered PS template was prepared using a method similar to the one described by Shen et al.[8] with modification. Styrene was thoroughly washed with 10 wt % NaOH solution (40 mL and three times) and deionized water (50 mL and five times) to remove the stabilizer. Then, 65 mL of the washed styrene were mixed with 500 mL of polyvinylpyrrolidone (PVP K-30) aqueous solution (4 mg/mL) in a 1 L triple-neck round-bottomed flask. The mixture was bubbled with nitrogen for 15 min and then heated at 75 °C using an oil bath for 30 min under mechanical stirring (240 rpm). After that, 50 mL of aqueous solution of $K_2S_2O_8$ (20 mg/mL) was added to the flask, and the mixture was left to react for 24 h at 75 °C and 240 rpm. After cooling down to room temperature, the produced 3D ordered PS template was collected by centrifuging at 10,000 rpm for 4.5 h and then dried overnight in an oven at 60 °C.

3.3.2. Synthesis of Single-Crystalline Ordered M-ZIF-8. M-ZIF-8 was prepared in a method similar to that described by Shen et al.[8] with modification. The 3D ordered PS template (prepared as described in Section 3.3.1) was soaked in ZIF precursor solution in methanol, consisting of 8.15 g of $Zn(NO_3)_2{\cdot}6H_2O$ and 6.75 g of 2-methylimidazole in 45 mL of anhydrous methanol. The mixture was degassed in a vacuum for 15−30 min to facilitate the filling of the interstitial spaces between the 3D colloidal spheres with the precursor solution. After that, the mixture was dried at 50 °C for 12 h and then soaked in 80 mL of $CH_3OH/NH_3{\cdot}H_2O$ (1:1 v/v) solution at room temperature (RT). This mixture was degassed in a vacuum for 15−30 min and then left to react at RT and atmospheric pressure for 24 h. The templates, which gradually broke into small pieces due to the growing stress of ZIF-8, were filtrated and dried in air. The PS templates, which were confined in the M-ZIF-8, were removed by soaking in 400 mL of two times over 24 h. Finally, the obtained white powder was dried overnight at 70 °C.

3.3.3. Synthesis of m-M-ZIF-8. 3.54 g of $FeCl_3$, 2.49 g of $FeCl_2{\cdot}4H_2O$, and 0.25 g of polyacrylic acid were simultaneously dissolved in 50 mL of deionized water. The pH value of the mixture solution was adjusted to 9.0 by adding $NH_3{\cdot}H_2O$. The resulting Fe_3O_4 nanoparticle black precipitate was then recovered using a magnet and washed with ethanol.

N-Fe_3O_4 and N-M-ZIF-8 were prepared according to the method described by Gao et al.[14] Briefly, 0.5 g of Fe_3O_4 or M-ZIF-8 was added to 100 mL of CH_3CH_2OH solution containing 8 mL of 3-aminopropyltrimethoxysilane and stirred at 60 °C for 7 h. The product was washed with ethanol and dried overnight at 25 °C. 10 mg of *N*-Fe_3O_4 were then added to 1 mL of 100 mM Tris−HCl buffer (pH 8.0) containing 50 mg of activated N-M-ZIF-8 glutaraldehyde. After stirring for 1 h at room temperature, the resulting m-M-ZIF-8 was recovered using a magnet and washed with deionized water and freeze-dried for 4 h.

https://doi.org/10.1021/acsomega.1c04601
ACS Omega 2022, 7, 274−280

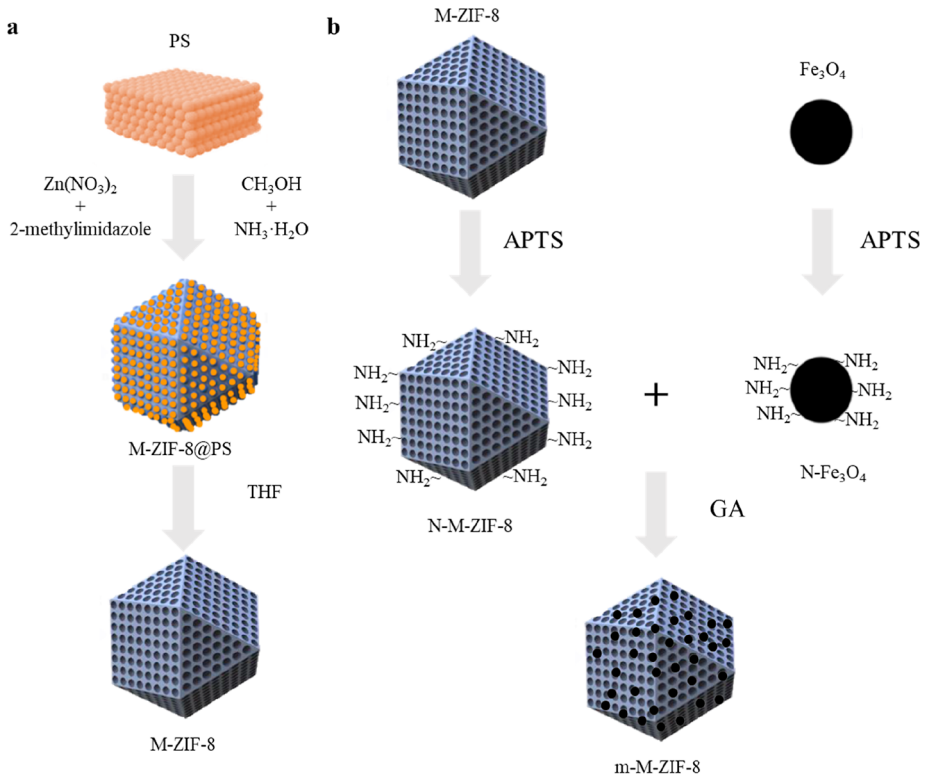

Figure 8. Synthesis procedure of (a) M-ZIF-8 and (b) m-M-ZIF-8.

3.3.4. Synthesis of C-ZIF-8. C-ZIF-8 was prepared according to the method described by Wu et al.[15] with modification. 1.47 g of Zn $(NO_3)_2{\cdot}6H_2O$ and 3.25 g of 2-methylimidazole were separately dissolved in 20 mL of methanol. Then, the two solutions were rapidly mixed in a glass beaker (100 mL); then, a white powdery solid was obtained after magnetic stirring for 3 h at 50 °C and 400 rpm. The solid product was centrifuged (4000 rpm, 5−10 min) and washed with methanol three times. Finally, the white ZIF-8 powder was dried in a vacuum drying oven overnight at 70 °C for 12 h.

3.3.5. Immobilization of TLL. To immobilize TLL inside the M-ZIF-8 and m-M-ZIF-8, 50 mg of M-ZIF-8 or m-M-ZIF-8 was added to 800 μL of 0.05 M Tris−HCl buffer (pH 7.0) in a 1.5 mL plastic centrifuge tube. After uniform dispersing of ZIF-8 by ultrasonication, 200 μL of soluble TLL solution was added, and the mixture was kept in a thermostatic shaker at 40 °C and 200 rpm for 4 h. The immobilized lipase was then collected by centrifugation, followed by vacuum filtration and freeze-drying process. Enzyme loading was calculated from the difference in protein concentration (measured using a BCA protein assay kit) in the original solution and what was left in the supernatant after the immobilization, as given by eq 1.

$$L(\text{enzyme loading}) = \frac{(C_0 - C_1) \times V}{m_s} \quad (1)$$

where C_0 and C_1 are the protein concentrations of the supernatant before and after the immobilization (mg/mL), respectively, V is the volume of total solution (1 mL), and m_s is the weight of ZIF (50 mg).

The procedures of synthesizing M-ZIF-8 and m-M-ZIF-8 are graphically presented in Figure 8.

3.3.6. Enzyme Activity Assay. The activity of free and immobilized lipase was determined by the butyrin hydrolysis method, as described in ref 18, using eq 2.

$$U = \frac{(V_1 - V_0) \times C_{\text{NaOH}} \times 10^3}{m_t \times t} \quad (2)$$

where, U is the specific activity (μmol•min^{-1}•mg^{-1}), with U_{hetero} and U_{free} representing the activity of the immobilized and free lipase, respectively, V_1 is the volume of NaOH titrated (mL) when lipase (free or immobilized) is used, V_0 is the titrated volume (mL) when the blank is used, C_{NaOH} is the concentration of sodium hydroxide (0.05M), m_t is the mass of free or immobilized lipase (mg), and t is the reaction time (10 min).

The activity recovery was then calculated using eq 3

$$R(\%) = \frac{U_{\text{hetero}} \times m_t}{U_{\text{free}} \times (L \times m_s \div \omega_f)} \times 100 \quad (3)$$

where R is the activity recovery, L is the enzyme loading amount, m_s is the weight of the support, and ω_f is the mass fraction of free enzyme in its solution. All data presented are average results of triplicated repetition of each run.

3.3.7. Lipase-Catalyzed Methanolysis of Soybean Oil. Enzymatic methanolysis of soybean oil was conducted in a 2 mL plastic centrifuge tube, which was placed in a thermostatic shaker at 40 °C and 200 rpm. The reaction conditions were as follows: 1 g of soybean oil, 0.1 g of deionized water, 120 U immobilized lipase per gram soybean of equal enzymatic activity, and four-step stepwise equal addition (at 0, 2, 4, and 6 h) of 46 μL of methanol. At the end of reaction (12 h), 100 μL of sample was withdrawn from the reaction mixture for analysis. The sample was first treated with a speed vacuum concentrator at 85 °C, 2000 rpm, and −0.1 MPa. Then, a

https://doi.org/10.1021/acsomega.1c04601
ACS Omega 2022, 7, 274−280

sample of 10 μL was added to 600 μL of heptadecanoic acid methyl ester ethanol solution (internal standard, 100 mg/100 mL), and 0.5 μL of the resulting mixture was injected in an Agilent 7890 gas chromatograph equipped with a CP-FFAP capillary column (0.32 mm × 0.30 μm×25 m). The initial column temperature was 180 °C which was maintained for 0.5 min and then heated to 250 °C at a rate of 10 °C/min and held for 6 min. The detector and injector were set at 250 °C and 245 °C, respectively. The FAME yield was calculated using eq 4:

$$Y(\text{FAME yield}) = \frac{m_i}{m_s} \times \frac{A_s}{A_i} \times 100\% \quad (4)$$

where m_i and m_s are the mass of the internal standard and sample, respectively, and A_i and A_s are the GC peak areas of the internal standard and FAMEs, respectively. All data presented are average results of triplicated repetition of each run.

3.3.8. Reusability Test of TLL@M-ZIF-8 and TLL@m-M-ZIF-8 in Methanolysis of Soybean Oil. The methanolysis reaction, similar to the one described in Section 3.3.5 was carried out, and 50 μL of the organic phase was withdrawn at 12 h and treated using a speed vacuum concentrator for gas chromatography (GC) analysis. After that, the reaction mixture was centrifuged at 6000 rpm for 5 min, and the immobilized enzyme was collected, washed three times with tertiary butanol, and then freeze-dried overnight. The recovered enzyme was reused for the next batch's methanolysis reaction. All presented data are the average values of triplicated runs.

4. CONCLUSIONS

m-M-ZIF-8 with a 3D highly ordered macroporous structure was successfully synthesized and explored for lipase immobilization for the first time. It was found that enzyme loading and the specific enzyme activity of the immobilized lipase were greatly enhanced through this magnetic modification. Most significantly, the magnetic modification made recycling of lipase more easy using a magnet and significantly enhanced the reusability of the immobilized lipase. This work provides an efficient path to immobilize enzymes on/in macroporous MOFs with enhanced reusability.

AUTHOR INFORMATION

Corresponding Authors

Sulaiman Al-Zuhair − *Department of Chemical and Petroleum Engineering, United Arab Emirates University, Al Ain 15551, UAE*; Email: s.alzuhair@uaeu.ac.ae

Wei Du − *Key Laboratory for Industrial Biocatalysis, Ministry of Education, Department of Chemical Engineering, Tsinghua University, Beijing 100084, China*; orcid.org/0000-0003-4094-210X; Email: duwei@tsinghua.edu.cn

Authors

Yuhan Li − *Key Laboratory for Industrial Biocatalysis, Ministry of Education, Department of Chemical Engineering, Tsinghua University, Beijing 100084, China*

Hao Zhou − *Key Laboratory for Industrial Biocatalysis, Ministry of Education, Department of Chemical Engineering, Tsinghua University, Beijing 100084, China*

Lingmei Dai − *Key Laboratory for Industrial Biocatalysis, Ministry of Education, Department of Chemical Engineering, Tsinghua University, Beijing 100084, China*

Dehua Liu − *Key Laboratory for Industrial Biocatalysis, Ministry of Education, Department of Chemical Engineering, Tsinghua University, Beijing 100084, China*

Complete contact information is available at: https://pubs.acs.org/10.1021/acsomega.1c04601

Author Contributions

Y.L.: conceptualization, methodology, software, validation, formal analysis, investigation, writing original draft, and writing review editing; H.Z.: conceptualization, resources, methodology, and software; L.D.: methodology and software; D.L.: project administration; S.Al-Z..: conceptualization, supervision, project administration, and funding acquisition; and W.D.: conceptualization, supervision, project administration, and funding acquisition.

Notes

The authors declare no competing financial interest.

ACKNOWLEDGMENTS

The authors express their gratitude for the support from the Joint Research Program between UAE University and Institutions of Asian Universities Alliance (AUA) (UAEU-AUA fund number 31R167) and Dongguan Science and Technology Bureau (Innovative R&D Team Leadership of Dongguan City, 201536000100033).

REFERENCES

(1) Liang, S.; Wu, X.-L.; Xiong, J.; Zong, M.-H.; Lou, W.-Y. Metal-organic frameworks as novel matrices for efficient enzyme immobilization: An update review. *Coord. Chem. Rev.* **2020**, *406*, 213149.

(2) Cui, J.; Ren, S.; Sun, B.; Jia, S. Optimization protocols and improved strategies for metal-organic frameworks for immobilizing enzymes: Current development and future challenges. *Coord. Chem. Rev.* **2018**, *370*, 22−41.

(3) Feng, Y.; Zhao, Y.; Ge, J. Impact of the size effect on enzymatic electrochemical detection based on metal-organic frameworks. *Anal. Chim. Acta* **2021**, *1149*, 238191.

(4) Wu, S.; Sun, Z.; Peng, Y.; Han, Y.; Li, J.; Zhu, S.; Yin, Y.; Li, G. Peptide-functionalized metal-organic framework nanocomposite for ultrasensitive detection of secreted protein acidic and rich in cysteine with practical application. *Biosens. Bioelectron.* **2020**, *169*, 112613.

(5) Hu, Y.; Zhou, H.; Dai, L.; Liu, D.; Al-Zuhair, S.; Du, W. Lipase Immobilization on Macroporous ZIF-8 for Enhanced Enzymatic Biodiesel Production. *ACS Omega* **2021**, *6*, 2143−2148.

(6) Fang, Q.-R.; Makal, T. A.; Young, M. D.; Zhou, H.-C. Recent advances in the study of mesoporous metal-organic frameworks. *Comments Inorg. Chem.* **2010**, *31*, 165−195.

(7) Xuan, W.; Zhu, C.; Liu, Y.; Cui, Y. Mesoporous metal-organic framework materials. *Chem. Soc. Rev.* **2012**, *41*, 1677−1695.

(8) Shen, K.; Zhang, L.; Chen, X.; Liu, L.; Zhang, D.; Han, Y.; Chen, J.; Long, J.; Luque, R.; Li, Y.; Chen, B. Ordered macro-microporous metal-organic framework single crystals. *Sci* **2018**, *359*, 206−210.

(9) Cheng, Y.; Ma, B.; Tan, C.-P.; Lai, O.-M.; Panpipat, W.; Cheong, L.-Z.; Shen, C. Hierarchical macro-microporous ZIF-8 nanostructures as efficient nano-lipase carriers for rapid and direct electrochemical detection of nitrogenous diphenyl ether pesticides. *Sens. Actuators, B* **2020**, *321*, 128477.

(10) Ricco, R.; Malfatti, L.; Takahashi, M.; Hill, A. J.; Falcaro, P. Applications of magnetic metal-organic framework composites. *J. Mater. Chem. A* **2013**, *1*, 13033−13045.

(11) Wang, D.; Zheng, P.; Chen, P.; Wu, D. Immobilization of alpha-L-rhamnosidase on a magnetic metal-organic framework to effectively improve its reusability in the hydrolysis of rutin. *Bioresour. Technol.* **2021**, *323*, 124611.

(12) Zou, Y.; Zhang, Y.; Liu, X.; Zhang, H. Solvent-Free Synthetic Fe_3O_4@ZIF-8 Coated Lipase as a Magnetic-Responsive Pickering Emulsifier for Interfacial Biocatalysis. *Catal. Lett.* **2020**, *150*, 3608−3616.
(13) Feng, Y.; Hu, H.; Wang, Z.; Du, Y.; Zhong, L.; Zhang, C.; Jiang, Y.; Jia, S.; Cui, J. Three-dimensional ordered magnetic macroporous metal-organic frameworks for enzyme immobilization. *J. Colloid Interface Sci.* **2021**, *590*, 436−445.
(14) Gao, F.; Pan, B.-F.; Zheng, W.-M.; Ao, L.-M.; Gu, H.-C. Study of streptavidin coated onto PAMAM dendrimer modified magnetite nanoparticles. *J. Magn. Magn. Mater.* **2005**, *293*, 48−54.
(15) Wu, C.-S.; Xiong, Z.-H.; Li, C.; Zhang, J.-M. Zeolitic imidazolate metal organic framework ZIF-8 with ultra-high adsorption capacity bound tetracycline in aqueous solution. *RSC Adv.* **2015**, *5*, 82127−82137.
(16) Hou, C.; Wang, Y.; Ding, Q.; Jiang, L.; Li, M.; Zhu, W.; Pan, D.; Zhu, H.; Liu, M. Facile synthesis of enzyme-embedded magnetic metal-organic frameworks as a reusable mimic multi-enzyme system: mimetic peroxidase properties and colorimetric sensor. *Nanoscale* **2015**, *7*, 18770−18779.
(17) Hu, Y.; Dai, L.; Liu, D.; Du, W. Hydrophobic pore space constituted in macroporous ZIF-8 for lipase immobilization greatly improving lipase catalytic performance in biodiesel preparation. *Biotechnol. Biofuels* **2020**, *13*, 86.
(18) Hu, Y.; Dai, L.; Liu, D.; Du, W. Rationally designing hydrophobic UiO-66 support for the enhanced enzymatic performance of immobilized lipase. *Green Chem.* **2018**, *20*, 4500−4506.

https://doi.org/10.1021/acsomega.1c04601
ACS Omega 2022, 7, 274−280